

5.8 Representative Examples

In this section some selected examples will be presented to illustrate the power of the proposed synthesis method for different array geometries as well as different kinds of pattern and excitation constraints. The power of the method in the synthesis of shaped beam equi-spaced linear arrays is already demonstrated in first three case studies. The ability to synthesise fixed nulls in conformal arrays is proven in the fourth case study as well as in Section 5.7.2 and Section 5.7.4.

The first example is a non-uniformly spaced linear array with a pencil beam to show the ability to synthesise non-uniformly spaced arrays. A circular arc array with a shaped beam pattern is synthesised for two different kinds of excitation constraints. The next two examples are planar arrays, one a planar array with a rectangular lattice in a circular boundary with a contoured footprint pattern; and the other a hexagonal array with a fan beam pattern. Lastly a fan beam pattern, spherical array with both co- and cross polarisation is presented.

In each example the information to reproduce the results will be listed:

- the array geometry will be described;
- followed by the specification of the radiation pattern requirements;
- next the excitation constraints, if any will be specified
- and the starting point selection will be described

Additional notes and a short discussion will conclude each example.

5.8.1 Example #1: Linear non equi-spaced array with a pencil beam

This example is the synthesis of a thinned or non-uniformly spaced linear array. This is a one dimensional array. The specification are:

- Geometry: Sixteen elements are removed from a 32 isotropic element equi-spaced linear array, with the inter element spacing of the original array $d = \frac{1}{2}\lambda$.
- Pattern specification: A pencil beam radiation pattern with the narrowest possible beam width for a required sidelobe level of -13dB .
- Excitation constraints: No excitation constraints imposed.
- Starting point: A single component beam in the broad side direction.

Since the array consist of isotropic elements the radiation pattern and the array factor is the same. The radiation pattern and excitation for this array in shown in Figure 5.11. For comparison two uniformly spaced arrays, one with the same number of elements ($N = 16$) and original array $N = 32$, with Dolph-Chebyshev distributions are also shown. The beamwidth of the thinned array is slightly less than the mean of the beamwidths of the reference Dolph-Chebyshev arrays. On the excitation plot one can see that the thinned array does not have any edge brightening, while both reference arrays do exhibit edge brightening.

The proposed synthesis method does not have any provision to select which elements must be removed, for that [145] was used as a guide.

5.8.2 Example #2: Circular arc array with a shaped beam and tapered sidelobe levels

The circular arc array is an one dimensional conformal array. With the array in the xy -plane, the pattern is of interest in the xy -plane and is a function of ϕ only. For this example a shaped beam pattern with non uniform sidelobe level topography is required.

- Geometry: 45 elements are positioned at equal angular increments in a 120° arc on an infinite cylinder with a radius of $R = 15,34\lambda$. This radius and spacing produce an element on an arc spacing of 0.73λ . The elements are axial slots with length 0.48λ and width 0.01λ , the element patterns are calculated using GTD.
- Pattern specification:
 - a $\text{csc}^2(\phi)$ shaped main beam from $\phi = -10^\circ$ to $\phi = 30^\circ$ with a peak-to-peak ripple of 1dB,
 - an inner sidelobe level from the main beam to $\phi = \pm 60^\circ$ of -25dB ,
 - sloping sidelobe envelope from -25dB at $\phi = \pm 60^\circ$ to -30dB at $\phi = \pm 150^\circ$,
 - and an outer sidelobe level from $\phi = \pm 150^\circ$ to $\phi = \pm 180^\circ$ of -30dB .
- Excitation constraints: Two different excitation constraints are imposed. Firstly the dynamic range (2.25) was interactively optimised and secondly the smoothness (2.26) was optimised.
- Starting point: Component beams with a nine variable phase function optimised with Genetic Algorithm was used for both cases.

The radiation patterns and excitation (amplitude only) for the two different sets of excitation constraints are displayed in Figure 5.12.

For the case where the dynamic range was optimised, the optimum dynamic range of $DR = 9.0$ was obtained; while the smoothness of this excitation is $S_m = 2.61$. On the

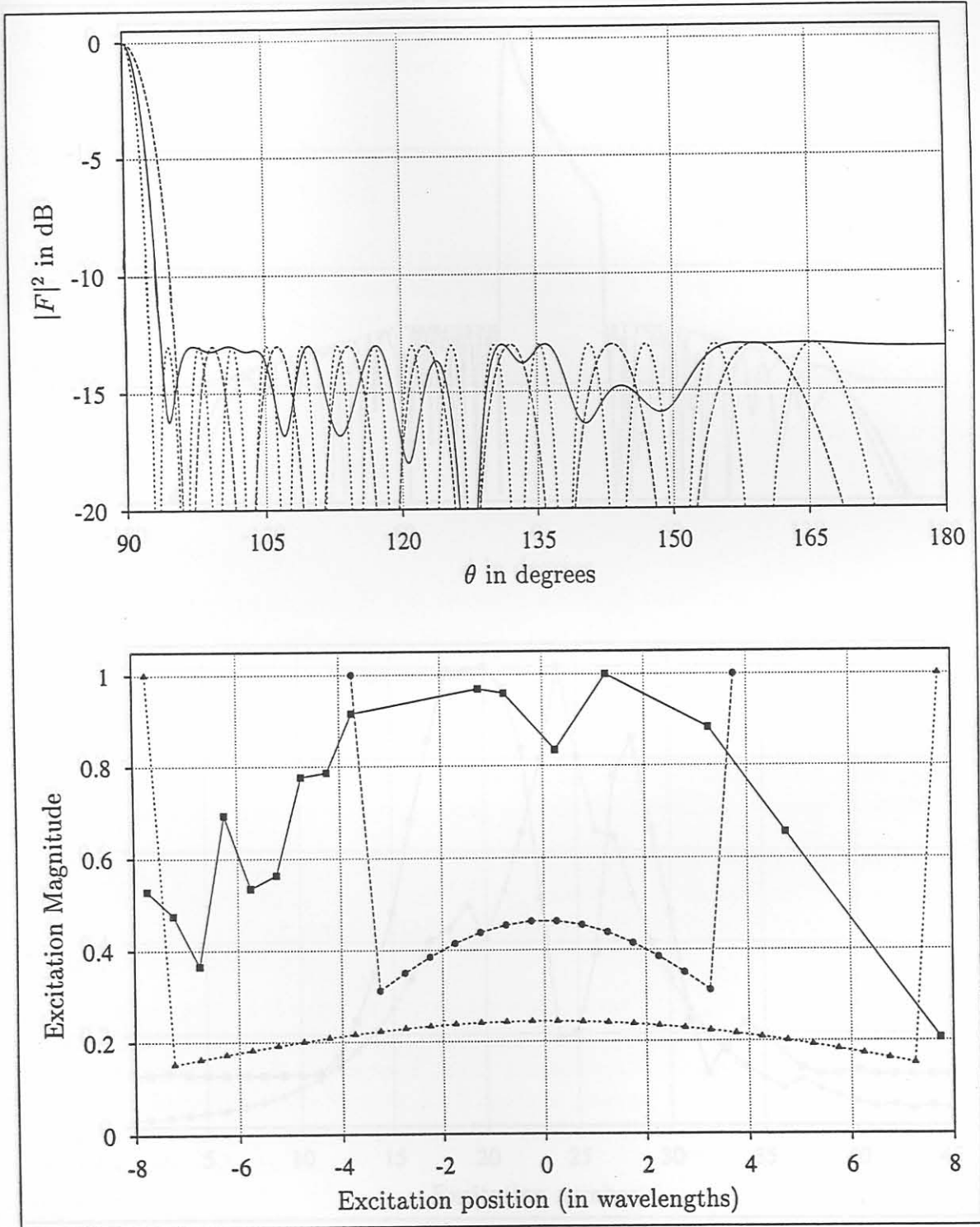


Figure 5.11: Example #1: The top graph show the radiation patterns of the thinned array (solid line) and the Dolph-Chebyshev distributions. The excitations of these arrays are displayed on the bottom graph using the same line types.

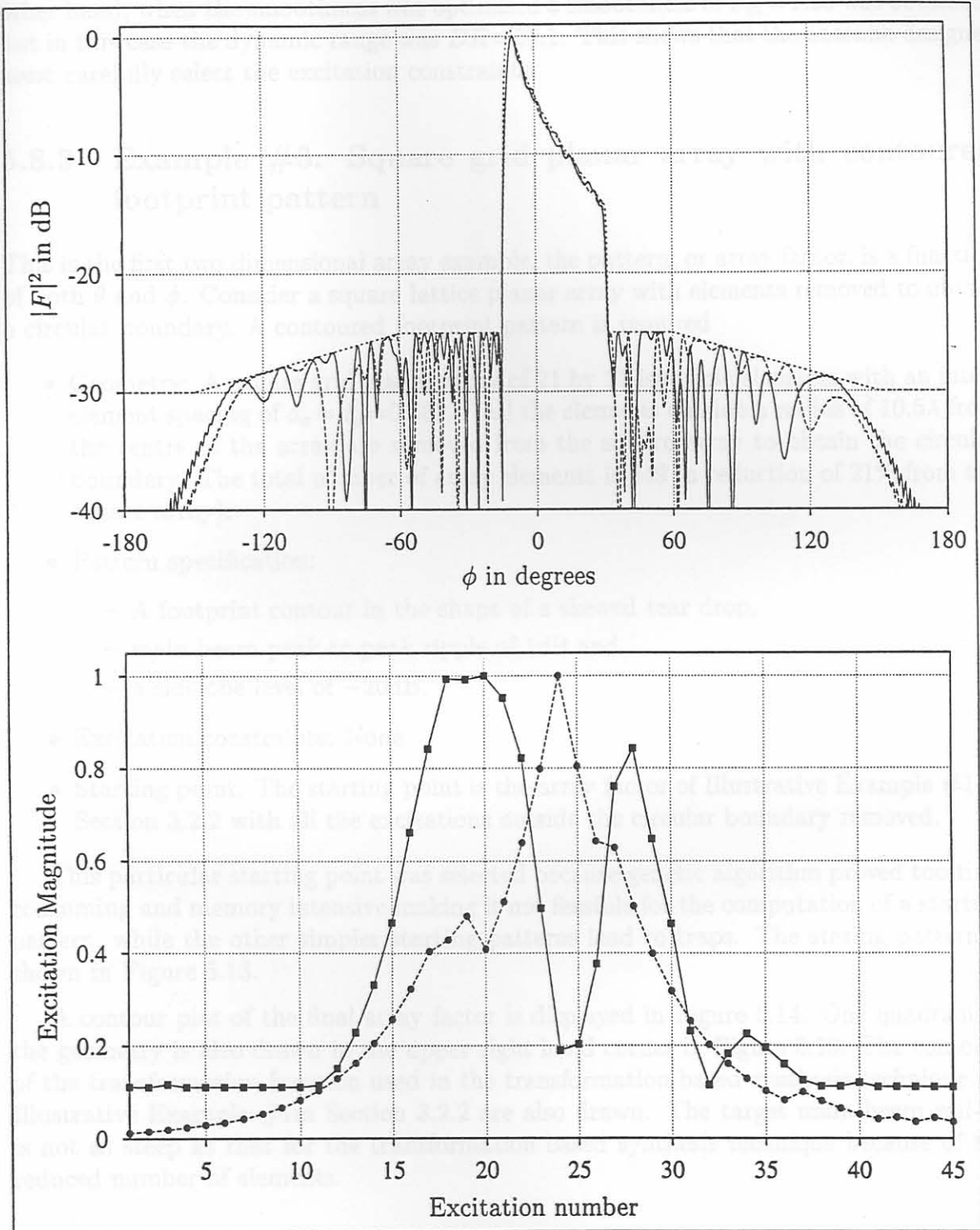


Figure 5.12: Example #2: The radiation patterns and excitations of the cylindrical arc arrays for the two different excitation constraints. The result with the dynamic range optimised is drawn by the solid traces and the result for the optimum smoothness is the dashed traces. The dotted curve represents the pattern mask.

other hand, when the smoothness was optimised a smoothness of $S_m = 1.26$ was obtained; but in this case the dynamic range was $DR = 83.1$. This shows that the antenna designer must carefully select the excitation constraints.

5.8.3 Example #3: Square grid planar array with contoured footprint pattern

This is the first two dimensional array example, the pattern, or array factor, is a function of both θ and ϕ . Consider a square lattice planar array with elements removed to obtain a circular boundary. A contoured footprint pattern is required

- **Geometry:** A square grid planar array of 21 by 21 isotropic elements with an inter-element spacing of $d_x = d_y = 0.662\lambda$. All the elements outside a radius of 10.5λ from the centre of the array are removed from the square array to obtain the circular boundary. The total number of array elements is 349 (a reduction of 21% from the square array).
- **Pattern specification:**
 - A footprint contour in the shape of a skewed tear drop,
 - main beam peak-to-peak ripple of 1dB and
 - a sidelobe level of -20 dB.
- **Excitation constraints:** None.
- **Starting point:** The starting point is the array factor of Illustrative Example #1 in Section 3.2.2 with all the excitations outside the circular boundary removed.

This particular starting point was selected because genetic algorithm proved too time consuming and memory intensive making it not feasible for the computation of a starting pattern, while the other simpler starting patterns lead to traps. The starting pattern is shown in Figure 5.13.

A contour plot of the final array factor is displayed in Figure 5.14. One quadrant of the geometry is also drawn in the upper right hand corner in Figure 5.13. The contours of the transformation function used in the transformation based synthesis technique for Illustrative Example #1 in Section 3.2.2 are also drawn. The target main beam roll-off is not as steep as that for the transformation based synthesis technique because of the reduced number of elements.

5.8.4 Example #4: Hexagonal planar array with a fan beam pattern

This example shows the performance of the intersection of sets synthesis method in shaped beam synthesis of a shaped beam hexagonal array.

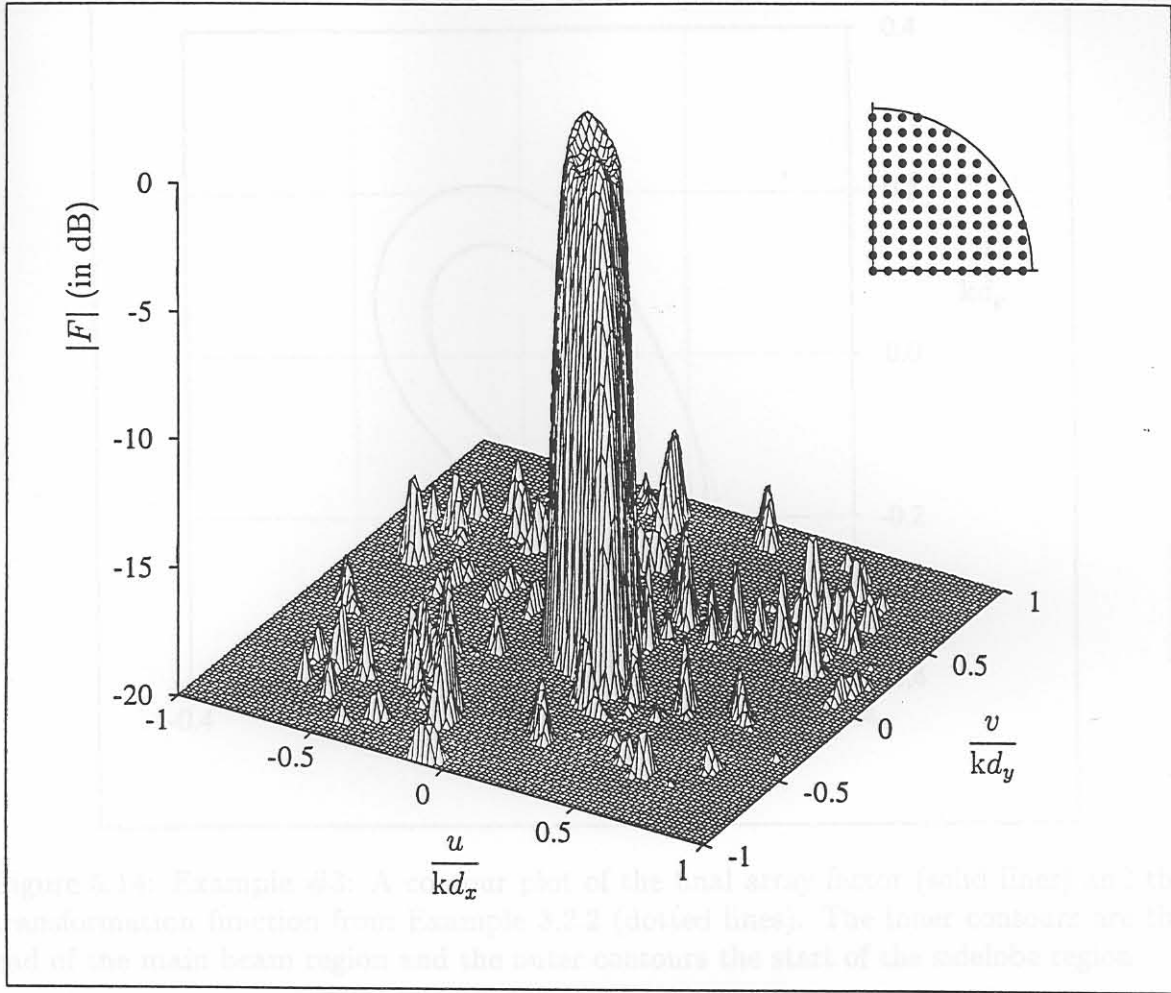


Figure 5.13: Example #3: A surface plot of the starting pattern, the planar array factor synthesised with the transformation based technique, with the corner elements removed.

- Geometry: A six ring hexagonal array with a total of 127 isotropic elements. The element spacing in the hexagonal lattice (shortest distance between any two elements) is $d_t = 0.577\lambda$. Thus the inter element spacing of collapsed distribution along the \hat{x} -axis is $d_x = \frac{1}{2}d_t = 0.288\lambda$ and that along the \hat{y} -axis is $d_y = d_t \sin(60^\circ) = \frac{1}{2}\lambda$.
- Pattern specification:
 - a $\text{csc}^2(\theta)$ shaped main beam from $\theta = -10^\circ$ to $\theta = 30^\circ \pm 1^\circ$ in the $\phi = 0^\circ$ -cut (along the \hat{x} -axis),
 - the narrowest pencil beam possible in the $\phi = 90^\circ$ -cut (along the \hat{y} -axis),
 - a peak-to-peak ripple of 2dB and
 - a sidelobe level of -20dB .
- Excitation constraints: None.

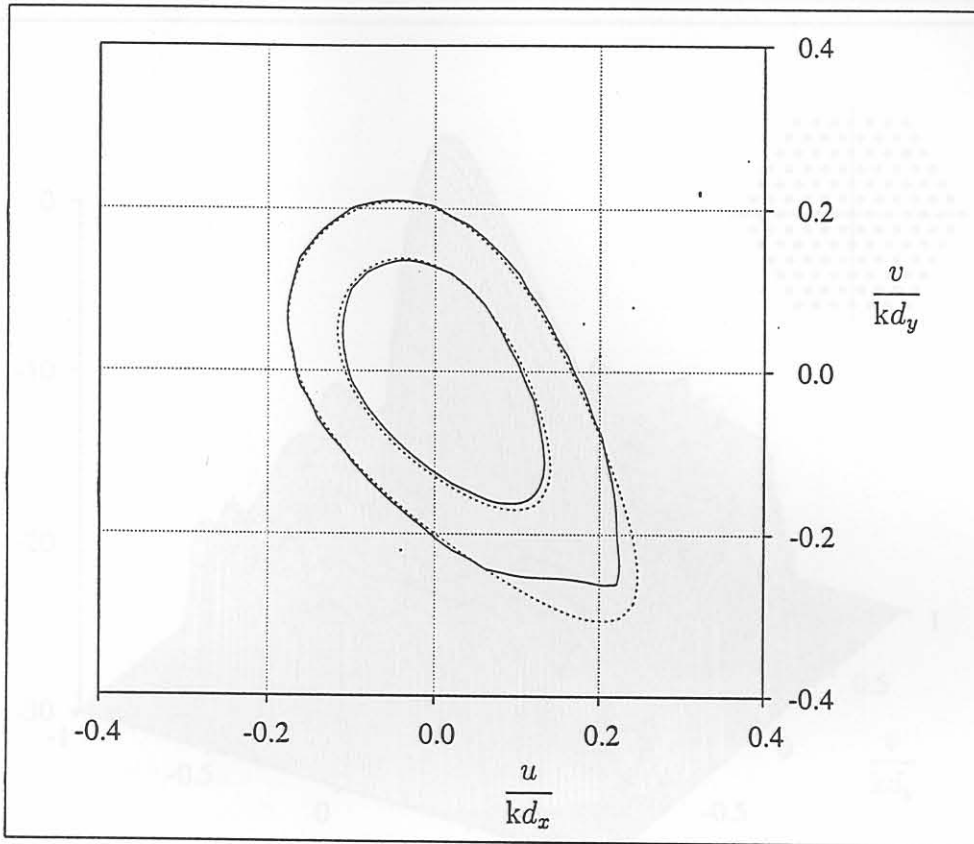


Figure 5.14: Example #3: A contour plot of the final array factor (solid lines) and the transformation function from Example 3.2.2 (dotted lines). The inner contours are the end of the main beam region and the outer contours the start of the sidelobe region.

- Starting point: Component beams with a seven parameter (one dimensional) phase function optimised with Genetic Algorithm.

The radiation pattern of the synthesised array is shown in Figure 5.15. Notice the circular sidelobe topography, this is indicative of a high excitation efficiency.

5.8.5 Example #5: Spherical array with simultaneous co- and cross polarisation pattern synthesis

In this example a full two dimensional conformal array (two pattern angles), on a spheroid with simultaneous co- and cross polarisation patterns is synthesised.

- Geometry:
 - Five rings of radiating elements on a spherical surface, a total of 91 elements.
 - The spherical surface has a radius of 10λ .

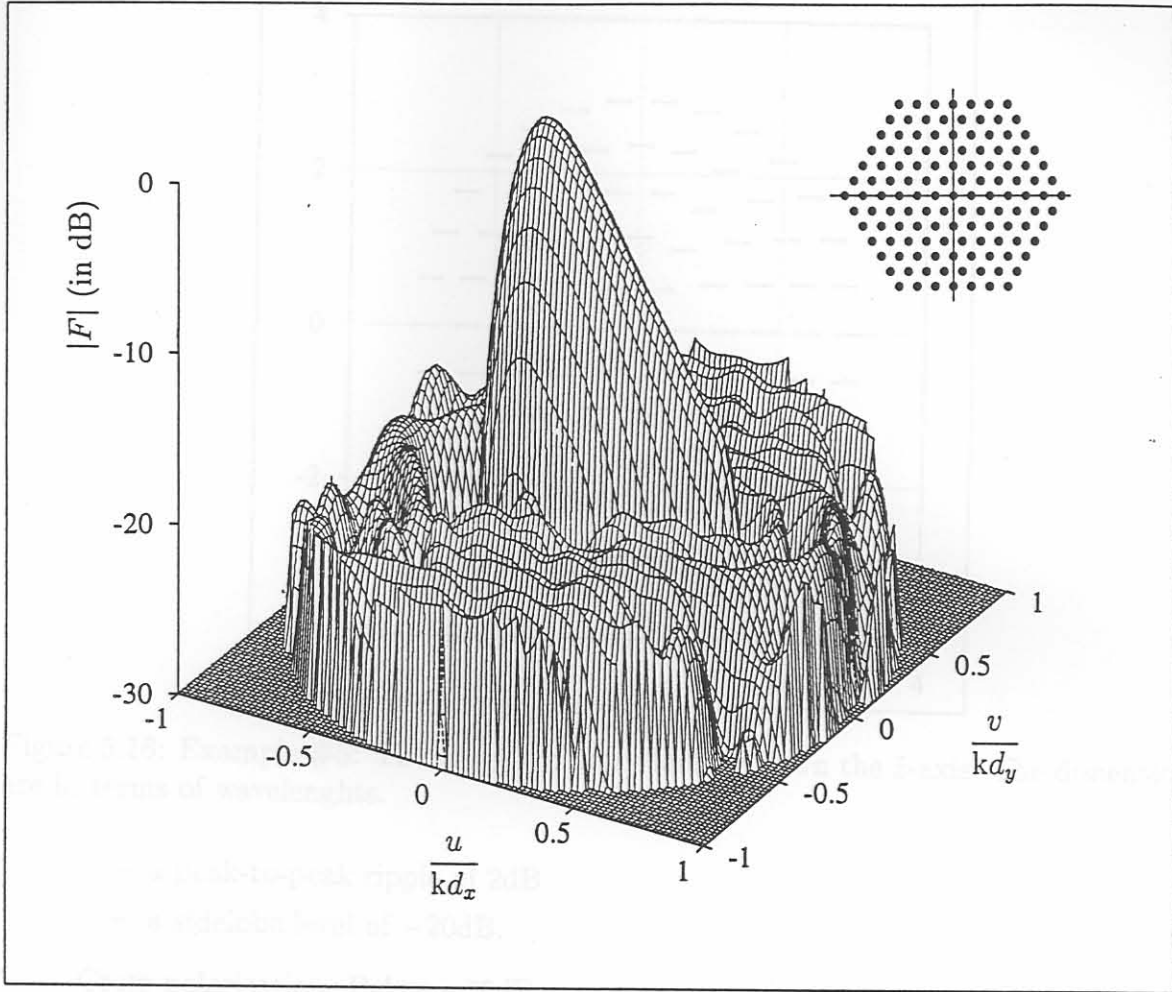


Figure 5.15: Example #4: A surface plot of the planar array factor of the hexagonal arrays with the array geometry in the upper right hand corner.

- Each of the concentric rings of elements is at a constant θ -angle. The θ angle increased with 3.44° for each new ring, thus the arc-radius of each ring increased by 0.6λ .
- The radiators are slots with length 0.48λ and width 0.01λ . Due to symmetry all the element patterns will be identical. The element pattern, both co- and cross polarisation, was calculated with GTD. The elements are oriented to obtain maximum co-polarisation in the broadside (\hat{z}) direction.

• Pattern specification:

Co-polarisation:

- a $\text{csc}^2(\theta)$ shaped main beam from $\theta = -10^\circ$ to $\theta = 30^\circ \pm 2^\circ$ in the $\phi = 0^\circ$ principal cut,
- the narrowest beamwidth possible in the $\phi = 0^\circ$ principal cut,

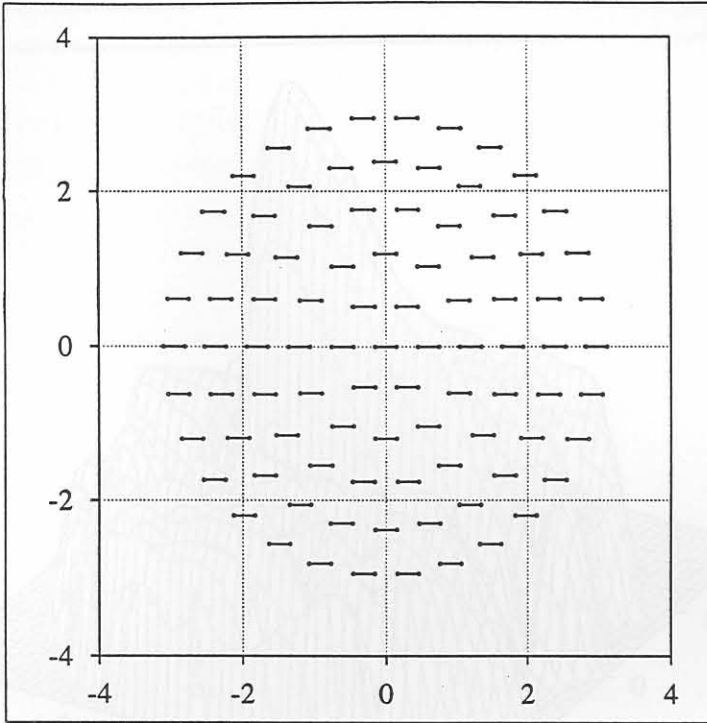


Figure 5.16: Example #5: The array geometry looking down the \hat{z} -axis. The dimensions are in terms of wavelengths.

- a peak-to-peak ripple of 2dB
- a sidelobe level of -20dB.

Cross polarisation: Below -30dB.

- Excitation constraints: None.
- Starting point: Component beams with a seven parameter (one dimensional) phase function optimised with Genetic Algorithm.

The geometry of the array, as seen looking down the \hat{z} -axis is drawn in Figure 5.16. The elements are oriented to get the best possible cross polarisation suppression in the bore sight ($\theta = 0^\circ$) direction. A surface plot of the final co-polarised radiation pattern is displayed in Figure 5.17. Again, notice the circular sidelobe topography, indicating a high excitation efficiency. Figure 5.18 show the radiation pattern in the $\phi = 0$ principal cut.

5.9 General Remarks and Conclusions

The synthesis of arrays of arbitrary geometry and elements can be stated as the search for the intersection of properly defined sets. Proper sets were defined in both the radiation

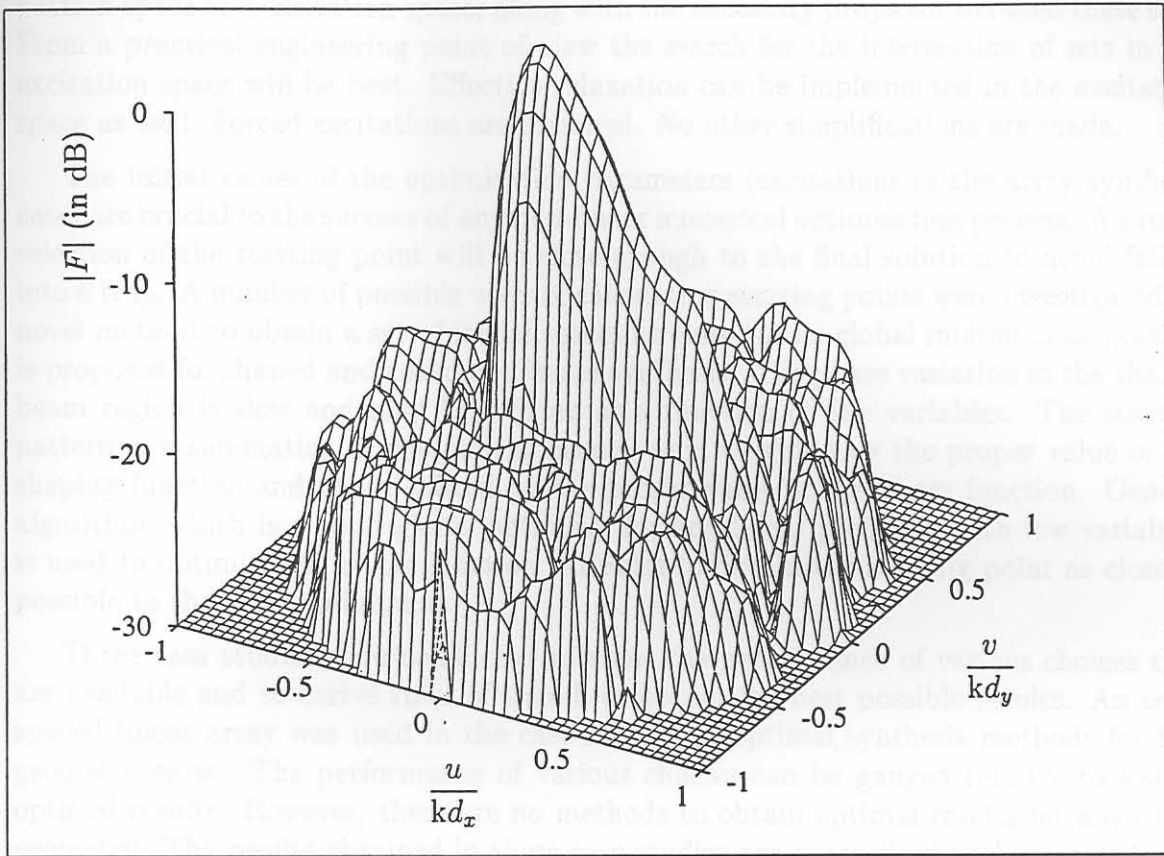


Figure 5.17: Example #5: A surface plot of the co-polarisation radiation pattern in the upper half space.

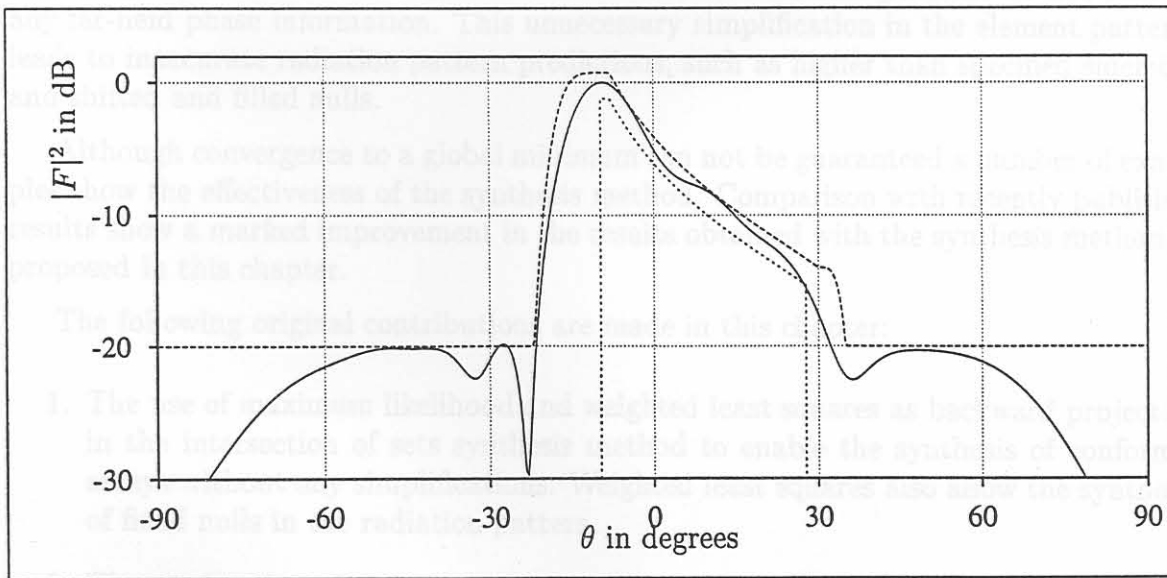


Figure 5.18: Example #5: The $\phi=0$ principal cut through the radiation pattern in the solid line trace, with the radiation pattern mask in dashed lines.

pattern space and excitation space; along with the necessary projector between these sets. From a practical engineering point of view the search for the intersection of sets in the excitation space will be best. Effective relaxation can be implemented in the excitation space as well. Forced excitations are assumed. No other simplifications are made.

The initial values of the optimisation parameters (excitations in the array synthesis case) are crucial to the success of any non-linear numerical optimisation process. A proper selection of the starting point will be close enough to the final solution to avoid falling into a trap. A number of possible ways of calculating starting points were investigated. A novel method to obtain a set of initial values as close to the global minimum as possible is proposed for shaped and contoured beam synthesis. The phase variation in the shaped beam region is slow and may be written as a function of few variables. The starting pattern is a summation of component beams, each weighted by the proper value of the shaping function and phase shifted by the proper value of the phase function. Genetic algorithm, which is a good global optimiser for non-linear problems with few variables, is used to optimise the phase function variables to obtain the starting point as close as possible to the global minimum.

Three case studies were conducted to show the performance of various choices that are available and to derive rules of thumb to obtain the best possible results. An equi-spaced linear array was used in the case studies as optimal synthesis methods for this geometry exist. The performance of various choices can be gauged relative to known optimal results. However, there are no methods to obtain optimal results for any other geometry. The results obtained in these case studies are generalised without proof, and should not be considered as more than rules of thumb.

The importance of practical element patterns in the analysis and synthesis of conformal arrays is shown. The analytical functions used for element patterns do not contain any far-field phase information. This unnecessary simplification in the element patterns leads to inaccurate radiation pattern predictions, such as higher than specified sidelobes and shifted and filled nulls.

Although convergence to a global minimum can not be guaranteed a number of examples show the effectiveness of the synthesis method. Comparison with recently published results show a marked improvement in the results obtained with the synthesis method as proposed in this chapter.

The following original contributions are made in this chapter:

1. The use of maximum likelihood and weighted least squares as backward projectors in the intersection of sets synthesis method to enable the synthesis of conformal arrays without any simplifications. Weighted least squares also allow the synthesis of fixed nulls in the radiation pattern.
2. The application of the generalised projection synthesis method in the excitation space. This ensures that all the excitation constraints necessary to implement the array are always satisfied. It also allows for the application of relaxation.

3. Effective relaxation in the excitation space as a convergence accelerator for slowly converging problems.
4. The importance of practical element patterns in the analysis and synthesis of conformal arrays is shown.
5. The component beam and radiation pattern phase function approach to obtain a starting point as close as possible to the global minimum to avoid traps.

The author published preliminary work on the proposed method [146].

Conclusions

A number of weaknesses in conventional array synthesis methods have been identified and addressed.

The transformation based synthesis method, prior to this thesis, could be used for the synthesis of rectangular planar arrays with quadrantal or plane symmetrical footprint patterns only. The transformation technique is extended to enable the synthesis of planar arrays with arbitrary contoured footprint patterns; planar arrays with non-rectangular boundaries and planar arrays with triangular lattices. The transformation based synthesis technique utilizes a transformation that divides the problem into two distinct sub-problems. One sub-problem (the contour transformation problem) involves the determination of certain coefficients in order to achieve the required footprint contour. The number of contour transformation coefficients which must be used depends on the complexity of the desired contour, but is very small in comparison to the number of planar array elements. The other sub-problem consists of a prototype linear array synthesis, for which powerful methods for determining appropriate element excitations, already exist. The separation of the synthesis procedure into two sub-problems is not only good from a computational point of view, but aids understanding by highlighting which contour features will finally determine the required array size (viz. contour complexity, allowed coverage ripple, local planar array directivity). Simple recursive formulas then determine the final planar array excitations from the information forthcoming from the above two sub-problem solutions. The final planar array size is limited to the number of contour transformation coefficients and the prototype linear array size. The biggest advantage of the transformation based synthesis technique is its computational efficiency, making it possible to conduct parametric studies of array performance design tradeoff studies even for very large arrays. However, the transformation based synthesis method does suffer some limitations. It can not be used to synthesise planar arrays with an arbitrary number of elements and it does not use all the degrees of freedom due to the very nature of the technique. Existing transformations were all shown to be special cases of the extended transformation based synthesis technique methods presented in the thesis.

No useful difference pattern synthesis method exists for planar arrays. A well ordered,